Single Molecule Atomic Force Microscopy Studies of Photosensitized Singlet Oxygen Behavior on a DNA Origami Template

Sarah Helmig,[†,‡] Alexandru Rotaru,[†,‡] Dumitru Arian,[§] Larisa Kovbasyuk,[§] Jacob Arnbjerg,[‡,⊥] Peter R. Ogilby,[‡,⊥] Jørgen Kjems,[†,¶] Andriy Mokhir,[§] Flemming Besenbacher,[†,#] and Kurt V. Gothelf[†,‡,*]

[†]Center for DNA Nanotechnology (CDNA) at the Interdisciplinary Nanoscience Center (iNANO), [‡]Department of Chemistry, Aarhus University, DK-8000 Aarhus C, Denmark, [§]Institute of Inorganic Chemistry, Ruprecht-Karls University, Heidelberg, Germany, and [⊥]Center for Oxygen Microscopy and Imaging, [¶]Department of Molecular Biology, and [#]Department of Physics and Astronomy, Aarhus University, DK-8000 Aarhus C, Denmark

ABSTRACT DNA origami, the folding of a long single-stranded DNA sequence (scaffold strand) by hundreds of short synthetic oligonucleotides (staple strands) into parallel aligned helices, is a highly efficient method to form advanced self-assembled DNA-architectures. Since molecules and various materials can be conjugated to each of the short staple strands, the origami method offers a unique possibility of arranging molecules and materials in well-defined positions on a structured surface. Here we combine the action of light with AFM and DNA nanostructures to study the production of singlet oxygen from a single photosensitizer molecule conjugated to a selected DNA origami staple strand on an origami structure. We demonstrate a distance-dependent oxidation of organic moieties incorporated in specific positions on DNA origami by singlet oxygen produced from a single photosensitizer located at the center of each origami.

KEYWORDS: DNA origami · singlet oxygen · AFM · single molecule imaging · photosensitizer

Arbitrary DNA origami structures containing typically 500000 atoms can be assembled with predesigned 1-, 2- or 3-dimensional shapes.[1−5] In our studies we have used a rectangular 2D DNA origami[1] adsorbed on a mica surface. This template can be applied for arranging proteins,[6−10] nanoparticles[11,12] and carbon nanotubes[14] with well-defined geometries. It offers an attractive opportunity to make single molecule studies of multicomponent systems using atomic force microscopy (AFM) since the individual components can be distinguished by their detailed position on the 100 × 70 nm^2 origami platform.

Previously, single molecule DNA hybridization assays[15] and protein affinity studies[16] have been reported and single molecule super resolution optical studies have been performed on a fluorophore-modified origami.[13] Furthermore, we recently showed that the DNA origami template can be used to study single molecule chemical reactions by AFM.[8]

Here, we use a DNA origami template to monitor aspects of singlet oxygen behavior, the latter having been produced upon irradiation of a single singlet oxygen photosensitizer molecule on the DNA origami surface.

Singlet oxygen ($^1O_2$) is the first electronically excited state of molecular oxygen and its physical and chemical properties have intrigued the scientific community for decades.[17,18] Singlet oxygen has a characteristic chemistry, which differs from that of the triplet ground state of oxygen, and includes specific oxygenation reactions of organic molecules. It is furthermore involved in a wide variety of biological processes, including events that result in cell death.[18]

To our knowledge, singlet oxygen has thus far only been monitored subsequent to its production from large populations of sensitizers. One possible exception stems from the work of Naito *et al.*[19] where singlet oxygen was generated photocatalytically at a TiO_2 surface and detected at the single-molecule level using a fluorescent probe. As such, the single molecule photosensitized work reported herein provides a unique perspective of singlet oxygen behavior.

In our current experiment, a single indium pyropheophorbide singlet oxygen photosensitizer[20] (IPS) is conjugated to a staple strand placed in the middle of the rectangular DNA origami (Figure 1, see Supporting Information for details).

To monitor the singlet oxygen produced at this point in space, we judiciously

*Address correspondence to kvg@chem.au.dk.

Received for review October 12, 2010 and accepted November 10, 2010.

Published online November 22, 2010. 10.1021/nn102701f

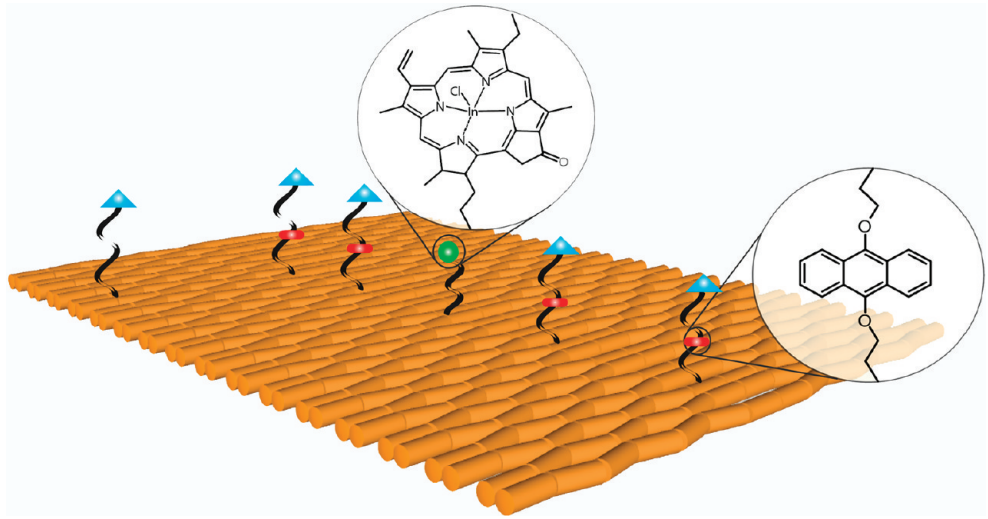

Figure 1. Schematic presentation of the origami structure with modified staple strands. The centrally positioned staple strand is modified with an IPS (green ball). The other 5 extended staple strands are modified with biotin (blue triangle). A $^1O_2$ cleavable (SOC) linker molecule (red rounded rectangle) is incorporated into the four staple strands positioned along the seam of the origami, whereas the remaining strand acts as a reference.

placed biotinylated oligonucleotides containing a singlet oxygen cleavable (SOC) linker in four positions on the origami surface (Figure 1). The $^1O_2$ sensitizer (IPS) and acceptors (SOC linkers) are thus completely separated spatially. A noncleavable biotinylated oligonucleotide was also positioned in the corner of the origami for reference.

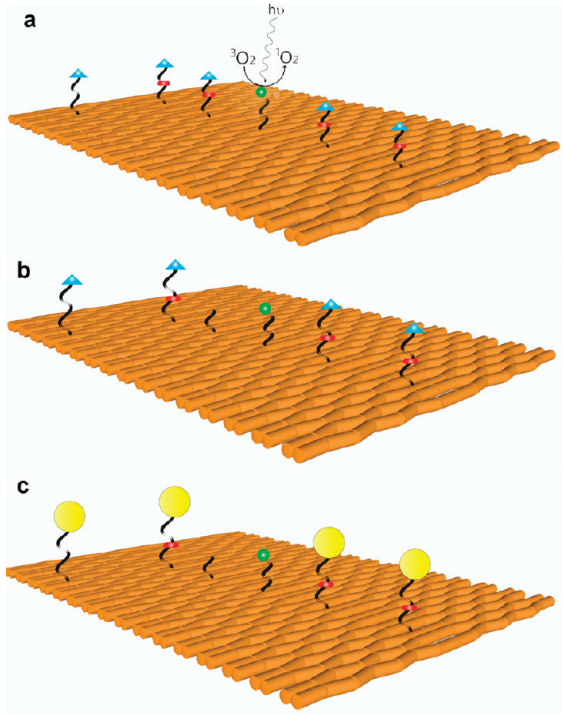

Figure 2. Schematic presentation of the molecular system. (a) Origami during irradiation; singlet oxygen is produced by the centrally positioned IPS and diffuses away from the IPS to react with the SOC linkers. (b) The result of a reaction with one of the SOC linkers is shown. Longer irradiation time results in cleavage of more SOC linkers. (c) Origami after irradiation and streptavidin addition. The remaining biotins are steptavidinated (yellow balls) and can thus be visualized with AFM.

The IPS is excited upon irradiation, and, because of the presence of molecular oxygen in the aqueous buffer covering the origami, the electronically excited IPS is quenched very efficiently in a process whereby energy is transferred from the excited state IPS to ground state oxygen to produce singlet oxygen. In this process, the IPS returns to its ground state and can thus be excited again and produce more singlet oxygen (Figure 2).

In an earlier study, we showed that the singlet oxygen-mediated cleavage of individual linkers incorporated into biotinylated origami staple strands can be monitored by AFM by binding streptavidin (SA) to the biotin moiety.[8] The biotin−SA complexes can easily be detected at nanoscale resolution since the streptavidins appear as bright protrusions in AFM images of the origami structures.[7,21,22] The linker used in our previous work[8,23] was, however, not cleaved efficiently enough to provide useful data for the current study involving a single singlet oxygen sensitizer. We thus employed a recently-developed more reactive SOC linker (Figure 1—see Supporting Information for details and Arian, D.; Kovbasyuk, L.; Mokhir, A. *A Fluorogenic Substrate for Monitoring Singlet Oxygen in Live Cells*. Submitted for publication).

Our present experiment, in which singlet oxygen produced in one highly localized spatial domain is detected by a specific reaction in a separate spatial domain, is, effectively, a single molecule analogue of the now classic experiment of Kautsky performed in 1931.[24] In the latter, a sensitizer bound to a solid phase support was physically separated from a reactive trap likewise bound to a solid phase support. The seminal point demonstrated by Kautsky was that singlet oxygen is a metastabile reactive species that can diffuse over an ap-

preciable distance before oxidizing a target substrate. In our present study, we show that one can now directly address nanoscale aspects of singlet oxygen diffusion in aqueous media. Our approach should have significant implications for the study of diffusion of singlet oxygen in biological systems, particularly for spatially resolved experiments performed at the level of a single cell.[18,25,26]

RESULTS AND DISCUSSION

The DNA origami was assembled by folding the bacteriophage M13mp18 single-stranded DNA genome of 7249 nucleotides in the presence of >200 DNA staple strands[1] and the six strands modified with SOC-biotin, the sensitizer, and the reference biotin, respectively (Figure 1). The origami solution was treated with a 0.1 μM streptavidin containing buffer for 2 h, followed by application of the solution to a mica surface. The surface was imaged by AFM (Figure 3a−d) to reveal well-formed rectangular origami, containing bright protrusions from the streptavidin, located exclusively in the five expected positions at the origami surface.

The yield of the streptavidin−biotin binding reaction is less than unity for each of the biotinylated positions, and therefore only few of the counted origamis contain all five streptavidins (Figure 3). Furthermore, the number of streptavidins at the origami decreases after continuous AFM imaging, as a result of the dynamic contact mode used in this procedure.

In our initial studies, the origamis were folded and incubated with streptavidin in solution, deposited on mica and imaged by AFM. Subsequently the immobilized origami were irradiated and imaged again by AFM.[8] This approach resulted in no observed cleavage, which may be a result of the new SOC linker being fully or partially embedded into the biotin binding pocket of streptavidin. In this case, we suggest that the generated singlet oxygen reacts with the protein rather than the embedded linker.[27] To circumvent this problem, the functionalized origami samples as illustrated in Figure 1 were dispersed in a solution of aqueous buffer and irradiated before the addition of streptavidin. Thereafter, streptavidin was added, and the samples were immobilized onto mica for AFM imaging. In this way, only noncleaved SOC-biotins are streptavidinated and imaged (Figures 2 and 3).

Of course, within the context of providing information about spatially resolved events, the success of this latter solution-based experimental approach depends intrinsically on the absence of pronounced (a) "cross-talk" between origami structures and (b) bending of a given structure. We address these points as our discussion proceeds.

Thus, in our experiment, the origami sample was formed in solution, excess staple strands were removed by filtration, and the solution was split into four samples A−D. Sample A was incubated with streptavidin directly after filtration, immobilized on mica, and imaged by AFM to provide a reference for the cleavage reaction. For sample B, the sensitizer was irradiated for 90 min followed by incubation with streptavidin and mica immobilization for AFM imaging. Sample C was treated as sample B but, before irradiation, a large excess of the IPS sensitizer was added to the solution. A fourth sample, D, in which there was no sensitizer present (internal or external) was prepared and treated like sample B. Analysis of the four samples was performed by noting the number and positions of streptavidins on each origami. Depending on the experiment, the number of origami examined ranged between 129 and 817. In correlation with earlier observations, 90−95% of the origami were found to be immobilized "face-up" on the mica surface.[1,8] The results are summarized in Table 1 and Figure 4.

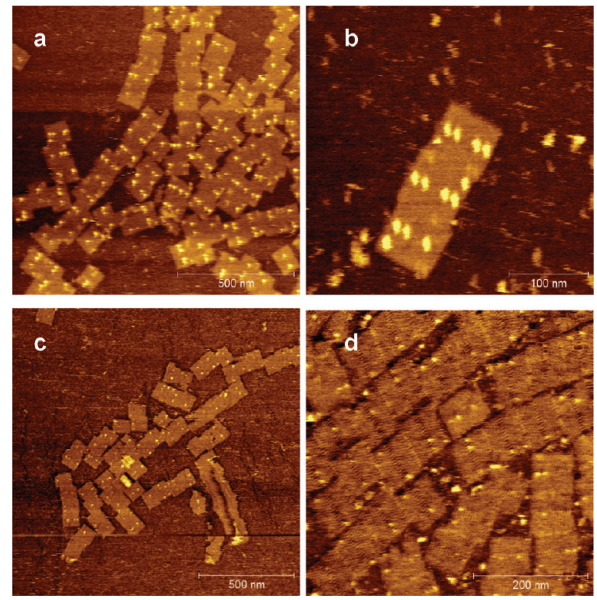

Figure 3. AFM images of origami with internal IPS: (a) overview of mica surface with origami that have not been irradiated; (b) three side-by-side origami, no irradiation; (c) overview of mica surface with origami after irradiation; (d) image of origami after irradiation with external IPS (10 μM) in solution.

Comparing the numbers obtained from samples A and B reveals that, as expected, the number of SOC-linked SAs decreases upon irradiation of the sensitizer. This indicates that the singlet oxygen-mediated cleavage reaction has occurred. In sample C, where IPS was also present in large excess in solution (10 μM), the subsequent AFM images revealed almost complete absence of streptavidins from the DNA origami surface.

TABLE 1. Data Obtained From AFM-Imaging of Samples A−D

sample	irradiation	IPS	origami counted	total SA	ref SA	SOC−SA
A	−	+	697	2319	597	1722
B	+	+	817	2288	693	1595
C	+	+	195	204	174	30
D	+	−	129	468	113	355

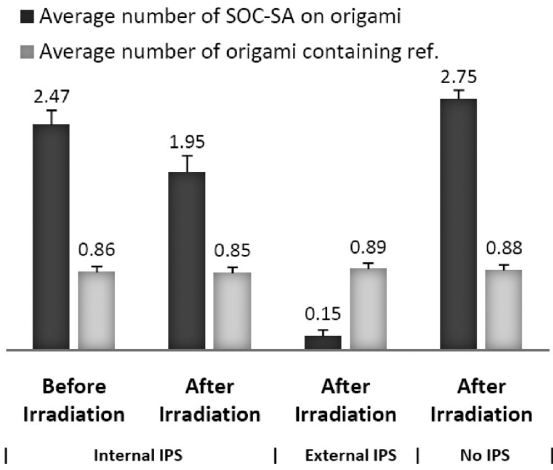

Figure 4. Graphical presentation of the average number of SAs in cleavable positions on each origami as well as the noncleavable reference point. Upon irradiation the number of SOC−SA is reduced, while the number of reference points remains the same.

In the absence of the IPS sensitizer (sample D) no decrease in the SA count was observed.

The average values of 2.47 SOC−SAs/origami before irradiation and of 0.86 ref-SAs/origami correspond to biotin−SA binding efficiencies that correlate well with previously observed efficiencies.[8] Note that the average value of 2.75 SOC−SA/origami observed for sample D, which contains no IPS, is higher than for sample A. Although the numbers 2.75 and 2.47 SOC−SAs/origami are arguably the same within our margin of error (Figure 4), this difference may also partly reflect the effects of spurious irradiation during the handling of sample A which contains the sensitizer.

The data obtained are consistent with the localized production of singlet oxygen at the center of a given origami, followed by the diffusion of singlet oxygen

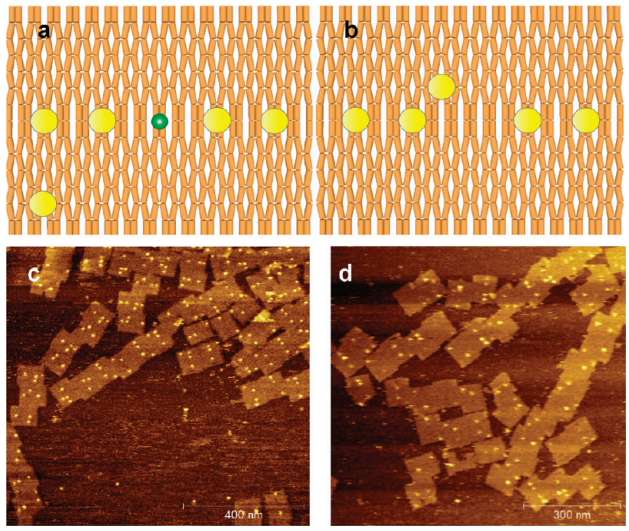

Figure 5. (a) Birds-eye schematic presentation of IPS origami; (b) schematic presentation of non-IPS origami; (c) AFM image of samples of mixed IPS- and non-IPS origami before irradiation. Origami of both designs are seen lying side-by-side; (d) AFM image of the sample after irradiation.

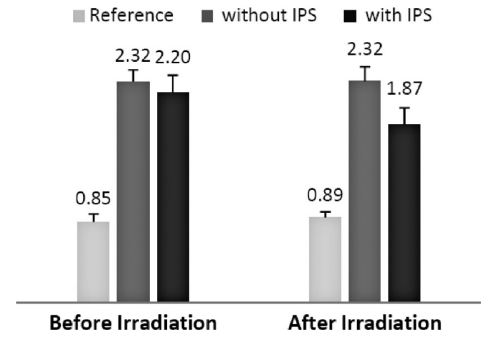

Figure 6. Graphical presentation of average SOC−SAs on IPS- and non-IPS origami before and after irradiation. The numbers for IPS origami and non-IPS origami refer to SOC−SA, while the reference point is noncleavable SA.

through the surrounding medium to the SOC linker. In an independent, time-resolved singlet oxygen phosphorescence experiment, we ascertained that in the aqueous buffer used, the lifetime of singlet oxygen did not differ appreciably from that in neat water (~4 μs). With this lifetime in mind, and assuming radial diffusion, we calculate that after a time period, t, of 12 μs (*i.e.*, 3 lifetimes, where ~5% of the original singlet oxygen population will remain), singlet oxygen will have diffused over a distance, d, of 380 nm (*i.e.*, $d = (6tD)^{1/2}$, where $D = 2 \times 10^{-5}$ cm^2 s^{-1} is the diffusion coefficient of oxygen in water).[28] Of course, any quenching of the singlet oxygen by the origami DNA will shorten the singlet oxygen lifetime and, hence, decrease the diffusion distance accordingly (see further discussion which follows).

For the origami templates used in our study, the distances from the $^1O_2$ sensitizer to the edges of the origami are 35 and 50 nm, respectively. Despite the fact that the 380 nm diffusion distance of singlet oxygen noted above is much larger than the dimension of a given origami, our experiments were performed at a sufficiently dilute origami concentration that singlet oxygen produced on one origami should not participate in the cleavage of SOC linkers on another origami. On the other hand, if origami aggregation occurs, one could indeed observe oxidative "cross-talk" between origamis.

To investigate the significance of this latter effect, IPS-free origamis were added to our system. These IPS-free samples were constructed such that the noncleavable biotinylated reference point was put in a different position, thereby allowing us to readily distinguish these samples in an AFM imaging experiment (Figure 5a−d).

As seen in Figures 5 and 6, cleavage of the linker clearly occurred on the IPS-containing structures, as expected, whereas there was no cleavage of linkers on the IPS-free structures. Thus, cross-talk between origami must not occur under our experimental conditions and, by inference, the origami do not aggregate such as to adversely affect our study.

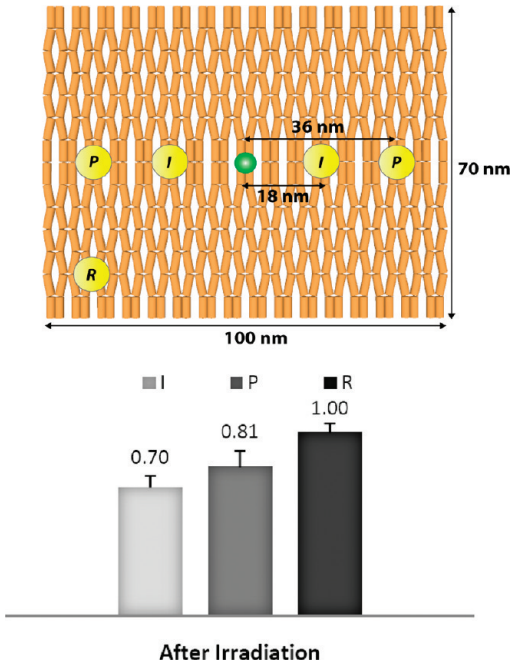

Figure 7. Top: Birds-eye schematic presentation of the streptavidinated origami structure. *I* = interior SOC−SA, *P* = peripheral SOC−SA, *R* = reference SA (noncleavable). Bottom: graphical presentation of the distance-dependent removal of SA on the origami. The data are normalized with respect to the number of SAs before irradiation.

For our experiments, which are performed under conditions of steady-state irradiation, we will produce a corresponding steady-state gradient of $^1O_2$ concentration which decreases as the distance from the IPS increases. Thus, the probability of singlet oxygen reacting with an SOC linker far away from the IPS should be less than that for an SOC linker close to the IPS. To investigate this, we compared the cleavage efficiency of the two interior SOC linkers located 18 nm from the IPS with the cleavage of the peripheral SOC linkers located 36 nm from the sensitizer (Figure 7 and Table 2).

As expected, the number of interior SOC−SAs remaining on the origami surface after irradiation of the sample is indeed less than the number of peripheral SOC−SAs. This is consistent with our model in which the cleavage reaction of the SOC linkers on a given origami involves singlet oxygen produced by the sensitizer on that same origami.

TABLE 2. Presentation of Data Obtained from Counting the Interior and Peripheral SAs

irradiation	origami counted	interior SOC−SA	peripheral SOC- SA	reference SA
−	594	723	683	509
+	578	491	537	493

Moreover, given that the interior and peripheral SOC linkers are, respectively, 18 and 36 nm away from the sensitizer, the corresponding fractions of SOC−SA removal of 0.7 and 0.8 for the interior and peripheral linkers, respectively, (Figure 7) point to a singlet oxygen lifetime that is somewhat less than the ~4 μs observed in the neat aqueous buffer. This is entirely expected given the fact that the DNA in the origami structure will quench singlet oxygen to some extent and thus shorten its effective radius of activity. Although the latter correlation is readily shown using a one-dimensional model for diffusion (*i.e.*, $d = (2tD)^{1/2}$), we are also assuming that, from a statistical perspective, data reflecting the effects of a "concave" bending of the origami platform will be offset by data reflecting the effect of "convex" platform bending. Thus, on average we can indeed treat the origami structure as a flat, rigid platform.

In summary, we have successfully developed a nanoscale multicomponent system for monitoring the reactions of singlet oxygen produced by a single photosensitizer using a DNA origami nanostructure as a platform. Most importantly, this system provides a spatially resolved tool by which one can quantify the extent to which singlet oxygen diffusion is manifested in the reactions of singlet oxygen with a given substrate.

EXPERIMENTAL SECTION

Formation of 2D DNA Origami. ***Preparation of Origami with IPS (Samples A, B, and C).*** The M13mp18 (New England Biolabs) scaffold strand solution was mixed with a 30 X excess of staple strands, including strands modified with biotin, SOC linker and biotin, or IPS to a final volume of 100 μL in a 2x Tris-acetate-EDTA (TAE) buffer with 12.5 mM $Mg(AcO)_2$ (pH = 8.2). The final concentration of the scaffold strand was 5 nM.

Assembly of the structure was accommodated by heating the solution rapidly to 65 °C and letting it cool down to 10 °C on an Eppendorf Mastercycler Personal machine over the course of 10 h. After annealing, the sample was purified by filtration (Amicon Ultra-0.5 100K centrifugal filters). After filtration the sample was split into three components, A, B, and C.

Preparation of Origami without IPS (Samples D and E). The origami was prepared following the above-mentioned procedure, except that H_2O was added instead of DNA-IPS solution. Annealing and purification was performed according to the normal procedure (*vide supra*). After filtration the sample was split into three, D_A, D_B, D_C/E_A, E_B, E_C. These samples were handled as samples A, B and C, respectively (*vide infra*).

Irradiation and Streptavidin Conjugation. Sample A was covered in tinfoil and 10 μM streptavidin solution was added to it, to a final SA-concentration of 0.1 μM. It was shaken at room temperature for 2 h.

Sample B was irradiated with either white light or 660 nm light from a custom-made LED array (Cetoni GmbH, Korbussen, Germany; 12 LEDs, $P = 2-4$ mW pr. LED), for 90 min, after which 10 μM streptavidin solution was added (final concentration = 0.1 μM) and the sample was shaken for 2 h.

A 500 nM IPS solution was added to sample C, to a final IPS concentration of 10 μM. The sample was hereafter treated like sample B.

Imaging and Analysis. A 5 μL drop of the sample was deposited onto a freshly cleaved mica surface (Ted Pella) and left to adsorb for 5 min. Buffer (1 × TAE · Mg^{2+}, 500 μL) was added to the liquid cell and the sample was scanned in a tapping mode using Agilent AFM series 5500 (Agilent Technologies) with silicon

nitride cantilevers (0.08 N/m force constant) with sharpened Pyramidal tip (OMCL-TR400PSA, Olympus, Atomic Force F&E GmbH). Several AFM images were obtained from separate locations across the mica surfaces to ensure reproducibility of the results. All the images were analyzed using Gwyddion 2.0 software.

Acknowledgment. This study was funded by the Danish National Research Foundation.

Supporting Information Available: Detailed experimental description, additional AFM images, detailed description and illustration of the image analysis method, DNA sequences, and structure of modifications. This material is available free of charge *via* the Internet at http://pubs.acs.org.

REFERENCES AND NOTES

1. Rothemund, P. W. K. Folding DNA to Create Nanoscale Shapes and Patterns. *Nature* **2006**, *440*, 297–302.
2. Andersen, E. S.; Dong, M.; Nielsen, M. M.; Jahn, K.; Lind-Thomsen, A.; Mamdouh, W.; Gothelf, K. V.; Besenbacher, F.; Kjems, J. DNA Origami Design of Dolphin-Shaped Structures with Flexible Tails. *ACS Nano* **2008**, *2*, 1213–1218.
3. Ke, Y.; Sharma, J.; Liu, M.; Jahn, K.; Liu, Y.; Yan, H. Scaffolded DNA Origami of a DNA Tetrahedron Molecular Container. *Nano Lett.* **2009**, *9*, 2445–2447.
4. Andersen, E. S.; Dong, M.; Nielsen, M. M.; Jahn, K.; Subramani, R.; Mamdouh, W.; Golas, M. M.; Sander, B.; Stark, H.; Oliveira, C. L.; *et al.* Self-Assembly of a Nanoscale DNA Box with a Controllable Lid. *Nature* **2009**, *459*, 73–76.
5. Douglas, S. M.; Dietz., H.; Liedl, T.; Högberg, B.; Graf, F.; Shih., W. M. Self-Assembly of DNA into Nanoscale Three-Dimensional Shapes. *Nature* **2009**, *459*, 414–418.
6. Yan, H.; Park, S. H.; Finkelstein, G.; Reif, J. H.; LaBean, T. H. DNA-Templated Self-Assembly of Protein Arrays and Highly Conductive Nanowires. *Science* **2003**, *301*, 1882–1884.
7. Kuzuya, A.; Kimura, M.; Numajiri, K.; Koshi, N.; Ohnishi, T.; Okada, F.; Komiyama, M. Precisely Programmed and Robust 2D Streptavidin Nanoarrays by Using Periodical Nanometer-Scale Wells Embedded in DNA Origami Assembly. *Chembiochem* **2009**, *10*, 1811–1815.
8. Voigt, N. V.; Torring, T.; Rotaru, A.; Jacobsen, M. F.; Ravnsbaek, J. B.; Subramani, R.; Mamdouh, W.; Kjems, J.; Mokhir, A.; Besenbacher, F.; *et al.* Single-Molecule Chemical Reactions on DNA Origami. *Nature Nanotechnol.* **2010**, *5*, 200–203.
9. Kuzyk, A.; Laitinen, K. T.; Torma, P. DNA Origami as a Nanoscale Template for Protein Assembly. *Nanotechnology* **2009**, *20*, 235305.
10. Endo, M.; Katsuda, Y.; Hidaka, K.; Sugiyama, H. Regulation of DNA Methylation Using Different Tensions of Double Strands Constructed in a Defined DNA Nanostructure. *J. Am. Chem. Soc.* **2010**, *132*, 1592–1597.
11. Pal, S.; Deng, Z. T.; Ding, B. Q.; Yan, H.; Liu, Y. DNA-Origami-Directed Self-Assembly of Discrete Silver-Nanoparticle Architectures. *Angew. Chem., Int. Ed.* **2010**, *49*, 2700–2704.
12. Ding, B. Q.; Deng, Z. T.; Yan, H.; Cabrini, S.; Zuckermann, R. N.; Bokor, J. Gold Nanoparticle Self-Similar Chain Structure Organized by DNA Origami. *J. Am. Chem. Soc.* **2010**, *132*, 3248–3249.
13. Steinhauer, C.; Jungmann, R.; Sobey, T. L.; Simmel, F. C.; Tinnefeld, P. DNA Origami as a Nanoscopic Ruler for Super-Resolution Microscopy. *Angew. Chem., Int. Ed.* **2009**, *48*, 8870–8873.
14. Maune, H. T.; Han, S. P.; Barish, R. D.; Bockrath, M.; Goddard, W. A.; Rothemund, P. W. K.; Winfree, E. Self-Assembly of Carbon Nanotubes into Two-Dimensional Geometries Using DNA Origami Templates. *Nat. Nanotechnol.* **2010**, *5*, 61–66.
15. Ke, Y. G.; Lindsay, S.; Chang, Y.; Liu, Y.; Yan, H. Self-Assembled Water-Soluble Nucleic Acid Probe Tiles for Label-free RNA Hybridization Assays. *Science* **2008**, *319*, 180–183.
16. Rinker, S.; Ke, Y. G.; Liu, Y.; Chhabra, R.; Yan, H. Self-Assembled DNA Nanostructures for Distance-Dependent Multivalent Ligand-Protein Binding. *Nat. Nanotechnol.* **2008**, *3*, 418–422.
17. Schweitzer, C.; Schmidt, R. Physical Mechanisms of Generation and Deactivation of Singlet Oxygen. *Chem. Rev.* **2003**, *103*, 1685–757.
18. Ogilby, P. R. Singlet Oxygen: There Is Indeed Something New under the Sun. *Chem. Soc. Rev.* **2010**, *39*, 3181–3209.
19. Naito, K.; Tachikawa, T.; Fujitsuka, M.; Majima, T. Real-Time Single-Molecule Imaging of the Spatial and Temporal Distribution of Reactive Oxygen Species with Fluorescent Probes: Applications to TiO_2 Photocatalysts. *J. Phys. Chem. C* **2008**, *112*, 1048–1059.
20. Arian, D.; Clo, E.; Gothelf, K. V.; Mokhir, A. A Nucleic Acid Dependent Chemical Photocatalysis in Live Human Cells. *Chem.—Eur. J.* **2010**, *16*, 288–295.
21. Winfree, E.; Liu, F. R.; Wenzler, L. A.; Seeman, N. C. Design and Self-Assembly of Two-Dimensional DNA Crystals. *Nature* **1998**, *394*, 539–544.
22. Li, H. Y.; Park, S. H.; Reif, J. H.; LaBean, T. H.; Yan, H. DNA-Templated Self-Assembly of Protein and Nanoparticle Linear Arrays. *J. Am. Chem. Soc.* **2004**, *126*, 418–419.
23. Rotaru, A.; Mokhir, A. Nucleic Acid Binders Activated by Light of Selectable Wavelength. *Angew. Chem., Int. Ed.* **2007**, *46*, 6180–6183.
24. Kautsky, H.; Bruijn, H. D. Die Aufklärung der Photoluminescenztilgung Fluorescierender Systeme durch Sauerstoff: Die Bildung aktiver, diffusionsfähiger Sauerstoffmoleküle durch Sensibilisierung. *Naturwissenschaften* **1931**, *19*, 1043.
25. Skovsen, E.; Snyder, J. W.; Lambert, J. D. C.; Ogilby, P. R. Lifetime and Diffusion of Singlet Oxygen in a Cell. *J. Phys. Chem. B* **2005**, *109*, 8570–8573.
26. Hatz, S.; Poulsen, L.; Ogilby, P. R. Time-Resolved Singlet Oxygen Phosphorescence Measurements from Photosensitized Experiments in Single Cells: Effects of Oxygen Diffusion and Oxygen Concentration. *Photochem. Photobiol.* **2008**, *84*, 1284–1290.
27. Davies, M. J. Singlet Oxygen-Mediated Damage to Proteins and Its Consequences. *Biochem. Biophys. Res. Commun.* **2003**, *305*, 761–770.
28. Tsushima, M.; Tokuda, K.; Ohsaka, T. Use of Hydrodynamic Chronocoulometry for Simultaneous Determination of Diffusion-Coefficients and Concentrations of Dioxygen in Various Media. *Anal. Chem.* **1994**, *66*, 4551–4556.